

SIMPLIFIED REACTION-DIFFUSION EQUATIONS FOR POTASSIUM AND CALCIUM ION CONCENTRATIONS DURING SPREADING CORTICAL DEPRESSION

HENRY C. TUCKWELL

Department of Mathematics, Monash University, Clayton, Victoria, Australia 3168

(Received June 11, 1980)

The reaction terms in the reaction–diffusion equations previously derived for the concentrations of potassium and calcium ions in brain structures during spreading depression are evaluated for various values of the ion concentrations. The null isoclines are estimated and the solitary wave trajectory plotted in the phase plane to find its relation to the isoclines and critical points of the kinetic equations. Four sets of simplified reaction terms are devised which have approximately the same dependence on the ion concentrations as those in the original system. The properties of the simplified equations are determined by numerical integration. Each system has a subthreshold response to a small local elevation of external K^+ concentration. The first, third and fourth systems support solitary wave solutions with properties similar to those of the original model system. Strength–duration curves are obtained and the response to a sustained stimulus evaluated. Collisions between waves are observed to result in their mutual destruction.

The phenomenon of spreading depression (SD) was first observed experimentally by Leao (1944) who noticed that electrical stimulation of rabbit neocortex could lead to a propagating depression of electroencephalographic activity which lasted locally for a few minutes with subsequent return to normal activity. Several years later it was demonstrated that SD was accompanied by the efflux of potassium ions (Brinley *et al.*, 1960) and more recent experiments have confirmed this fact (Vyskocil *et al.*, 1972; Nicholson *et al.*, 1977; Nicholson *et al.*, 1978; Kraig & Nicholson, 1978; Nicholson & Kraig, 1980). It has also been found that whilst the potassium ion concentration in the extracellular compartment of brain tissue increases, the concentrations of calcium ions, sodium ions and chloride ions decrease during SD. As the SD wave leaves a particular region, the ion concentrations return, sometimes somewhat slowly, to their resting values.

Apart from ion concentration changes there are many concomitant effects during SD. Efflux of

glutamate has been observed in the chicken retina (Van Harreveld & Fifkova, 1973) and increased metabolic activity monitored fluorimetrically in cat and rabbit neocortex (Rosenthal & Somjen, 1973; Mayevsky & Chance, 1974). Slow surface–negative potential waves occur of amplitude about 10–15mV, and neurons and glia undergo depolarization with neurons firing rapidly at early stages of the depolarization (Higashida *et al.*, 1974; Sugaya *et al.*, 1975). The wave of ion fluxes, depolarization and neuronal firing pattern moves across the cortical structure at a speed of about 3 mm/min.

A mathematical model for the temporal and spatial dependence of ion concentrations during spreading depression has been derived and analyzed (Tuckwell & Miura, 1978; Tuckwell, 1980a). The model consisted of a system of reaction–diffusion equations whose components were the extracellular and intracellular ion concentrations. There are many source and sink terms in a complete model for spreading depression, but when one takes into account only ion fluxes expected due to transmitter release, in the absence of action potentials, at depolarized synapses and active transport, the equations and calcium ion concentrations may be written,

I thank Davis Cope for many stimulating and helpful discussions and Betty K. Lang for technical assistance. This work was supported in part by National Research of Canada Grants A4559 and A9259.

$$K_t^0 = D_1 K^0_{xx} + k_1 g(V)(V - V_{Ca})(V - V_K) - k_2(1 - \exp[-k_3\{K^0 - K_{R^0}\}]), \quad (1a)$$

$$K_t^i = -k[k_1 g(V)(V - V_{Ca})(V - V_K) - k_2(1 - \exp[-k_3\{K^0 - K_{R^0}\}])], \quad (1b)$$

$$Ca_t^0 = D_2 Ca^0_{xx} + k_4 g(V)(V - V_{Ca}) + k_5(1 - \exp[-k_6\{Ca^i - Ca_{R^i}\}]), \quad (1c)$$

$$Ca_t^i = -k[k_4 g(V)(V - V_{Ca}) + k_5(1 - \exp[-k_6\{Ca^i - Ca_{R^i}\}])], \quad (1d)$$

where K^0 , K^i , Ca^0 , Ca^i are the extracellular and intracellular concentrations of potassium and calcium ions. Note that this is a reduced system—a complete set of model equations has recently been derived in which the components are the four ionic concentrations (K^+ , Ca^{++} , Na^+ , Cl^-) and excitatory and inhibitory transmitter concentrations (Tuckwell, in press). The quantities D_1 and D_2 are the diffusion coefficients for potassium and calcium ions in the extracellular space, $\{k_i\}$, $i = 1, \dots, 6$, are constants, K_{R^0} and Ca_{R^i} are the resting values of the extracellular potassium and intracellular calcium ion concentrations and k is the ratio of the extracellular to intracellular volumes within the tissue. The potentials are the membrane potential,

$$V = 58 \log_{10}[(K^0 + k_7)/k_8], \quad (2a)$$

under the assumption of fixed sodium and chloride ion concentrations, the potassium equilibrium potential,

$$V_K = 58 \log_{10}(K^0/K^i), \quad (2b)$$

and the calcium equilibrium potential,

$$V_{Ca} = 29 \log_{10}(Ca^0/Ca^i). \quad (2c)$$

The quantities k_7 and k_8 are further constants, containing the resting levels of Na^+ and Cl^- and their relative permeabilities (see Tuckwell, 1980a, for a discussion of the effects of regarding these as fixed).

The function $g(V)$ in Eqs. (1a)–(1d) indicates the dependence of calcium ion conductance (in particular for presynaptic membrane) on membrane potential. From available experimental evidence at squid giant synapse (Llinas *et al.*, 1976) and rat neuromuscular junction (Quastel, 1974) this dependence can be represented by

$$g(V) = [1 + \tanh\{k_9(V + V_T)\}]H(V - V^*), \quad (3)$$

where k_9 is a constant, V_T is a constant threshold type voltage and V^* is a constant cutoff voltage to ensure that there are no sources for K^+ and sinks for Ca^{++} close to resting levels, $H(\cdot)$ being the unit step function. The function $g(V)$, which is proportional to the actual conductance, is sketched in Figure 1 to show the meaning of the voltages V_T and V^* .

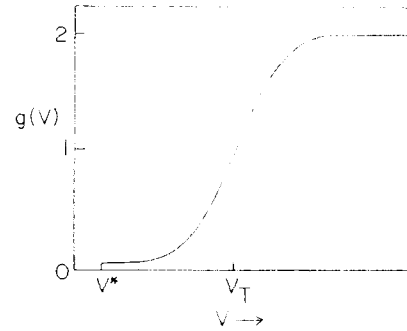


FIGURE 1 The form of the function $g(V)$ which approximates the variation in calcium conductance of presynaptic membrane with depolarization for the range of depolarizations encountered in spreading depression in the absence of action potentials.

In order to reduce the system of four Eqs. (1a)–(1d) to a two component system one can assume that for small amplitude waves (such as occur in TTX treated cortex) that the internal potassium ion concentration is fixed and further that the calcium concentrations inside and outside of cells are related by

$$Ca^i(x, t) = Ca_{R^i} + k[Ca_{R^0} - Ca^0(x, t)], \quad (4)$$

which is a local conservation condition. A comparison of results obtained under condition (4) with those when it is relaxed shows that it leads to only minor quantitative differences.

For notational convenience we set $u(x, t) = K^0(x, t)$ and $v(x, t) = Ca^0(x, t)$, so that the two component system is

$$u_t = D_1 u_{xx} + F(u, v), \quad (5a)$$

$$v_t = D_2 v_{xx} + G(u, v). \quad (5b)$$

where the reaction terms are

$$F(u, v) = d_1 h(u) [V(u) - V_{Ca}(v)] [V(u) - V_K(u)] - d_2 (1 - \exp[-d_3 \{u - u_0\}]), \quad (5c)$$

$$G(u, v) = d_4 h(u) [V(u) - V_{Ca}(v)] + d_5 (1 - \exp[-d_6 \{v_0 - v\}]). \quad (5d)$$

where $d_i, i = 1, \dots, 6$, are constants and u_0, v_0 are the resting levels of potassium and calcium ions in the extracellular space. Furthermore,

$$V(u) = 58 \log_{10}[(u + d_7)/d_8], \quad (6a)$$

$$V_K(u) = 58 \log_{10}(u/d_9), \quad (6b)$$

$$V_{Ca}(v) = 29 \log_{10}[v/(d_{10} - kv)], \quad (6c)$$

and the function $h(\cdot)$ is

$$h(u) = [1 + \tanh\{d_{11}(V(u) + V_T)\}]H(u - u^*). \quad (7)$$

Here u^* is the value of u such that $V(u^*) = V^*$ and d_7, \dots, d_{11} are constants.

The system of Eqs. (5)–(7) predicts very closely the same behaviors of the ionic concentrations as the system (1)–(3). In particular the initial conditions

$$u(x, 0) = u_0 + 8 \exp[-((x - 0.5)/0.025)^2], \quad (8a)$$

$$v(x, 0) = v_0. \quad (8b)$$

with $x \in (0, 1)$, representing a local elevation of potassium and resting level for calcium, lead to solitary waves consisting of increased K^+ and decreased Ca^{++} moving outward from the center of the stimulus. Details of the results of computations for various parameter values have been given previously (Tuckwell, 1980a).

The four component system, (1)–(3), and the two component system, (5)–(7), have complicated reaction terms involving logarithmic and exponential functions which make analysis difficult. Even the simpler system has 14 parameters so that it is desirable to obtain a two component system which has the same properties and fewer parameters with reaction terms which are polynomials. In total, four such two component systems will be examined and their properties ascertained by numerical integration.

DERIVATION OF THE SIMPLIFIED MODEL EQUATIONS

The reaction terms $F(u, v)$ and $G(u, v)$ of Eqs. (5c) and (5d) were evaluated for values of u between 2 and 25 mM and for values of v between 0.01 and 1 mM. The following values of the constants were employed: $d_1 = -0.75, d_2 = 52, d_3 = 10, d_4 = 0.075, d_5 = 0.52, d_6 = 10, d_7 = 9, d_8 = 180, d_9 = 140, d_{10} = 0.3, d_{11} = 0.11, k = 0.25, u_0 = 2, v_0 = 1, V_T = 45$ and $u^* = 2.2$. Those parts of the (u, v) -plane of relevance where $F(u, v)$ and $G(u, v)$ are positive or negative were thus found and the null isoclines ($F = 0$ or $G = 0$) and critical points ($F = 0$ and $G = 0$) of the system of ordinary differential equations $du/dt = F(u, v)$ and $dv/dt = G(u, v)$ were estimated by graphical techniques. These results are shown in Figure 2 where the critical points are labelled R (resting levels), A and B.

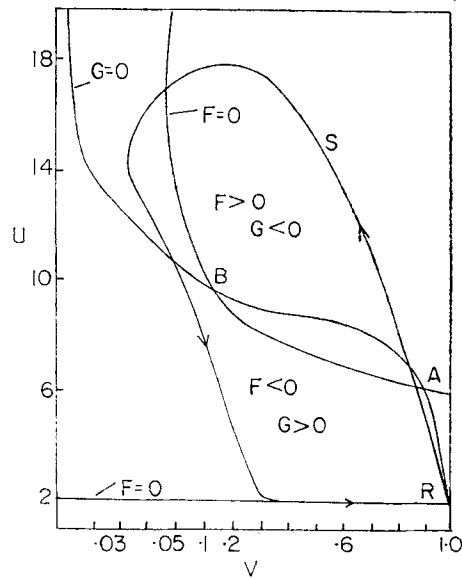


FIGURE 2 The regions of the (u, v) -plane at which $F(u, v)$ and $G(u, v)$ as in Eqs. (5) are positive or negative. The scale for v is divided into three linear regions. The curve marked S is the solitary wave trajectory for this system and the critical points for the kinetic equations are marked A, B and R (resting point).

Solutions of the reaction-diffusion system (5)–(7) were computed by the implicit Crank-Nicolson method with modification to allow for

the nonlinear terms due to Lees (1969). With the above values of the constants, $D_1 = 0.0025$, $D_2 = 0.00125$, the initial data of Eqs. (8a) and (8b) and boundary conditions $u(0, t) = u(1, t) = u_0$, $v(0, t) = v(1, t) = v_0$, stable solitary waves were obtained consisting of increased potassium ion concentration and depressed calcium ion concentration. As the two component solitary wave passes a given point in space, a temporal sequence of (u, v) pairs occurs at that space point which commences and ends at $R = (u_0, v_0)$. This sequence of points is plotted in the (u, v) plane and is marked as curve S (solitary wave trajectory) in Figure 2.

In order to construct the simplified model equations a pair of reaction terms $F(u, v)$ and $G(u, v)$ is sought for use in the system

$$u_t = D_1 u_{xx} + F(u, v), \quad (9a)$$

$$v_t = D_2 v_{xx} + G(u, v), \quad (9b)$$

such that the functions $F(u, v)$ and $G(u, v)$ are positive and negative at about the same parts of the (u, v) plane as the reaction terms of Eqs. (5c) and (5d). It is also required that the new reaction terms are such that the same number and relative positions of the critical points A, B and R, occur in the new and old systems.

Model 1

The first model considered is with null isoclines as shown in Figure 3A. Here $F = 0$ along the straight line $u = u_0$ and on the parabola through (u_2, v_2) and (u_4, v_0) , whereas $G = 0$ along the straight lines through (u_0, v_0) which also pass through (u_2, v_2) and (u_3, v_3) . The line RB is chosen to intersect the parabola twice.

The reaction terms are constructed as follows. The function $F(u, v)$ is chosen at fixed v to be a quadratic function of u such that it has zeros at $u = u_0$ and on the parabola through A and B and is negative between these values. This gives

$$F_1(u, v) = \alpha_1(u - u_0) [u - c_1(v - v_0)^2 - u_4], \quad (10)$$

where

$$c_1 = (u_2 - u_4)/(v_2 - v_0)^2, \quad (11)$$

and α_1 is a constant.

The function $G(u, v)$ is chosen at fixed u to be a parabola which is negative between the corresponding values of v on the straight lines RB and

RC and is positive outside this domain. This gives

$$G_1(u, v) = \beta_1(v - c_2u - c_3) [v - v_0 - c_4(u - u_0)], \quad (12)$$

where

$$c_2 = (v_3 - v_0)/(u_3 - u_0), \quad (13)$$

$$c_3 = v_3 - u_3(v_3 - v_0)/(u_3 - u_0), \quad (14)$$

$$c_4 = (v_2 - v_0)/(u_2 - u_0), \quad (15)$$

and β_1 is a constant.

Model 2

The same qualitative values of $F(u, v)$ and $G(u, v)$ occur as in the original system (Figure 2) if the restriction that $G(u, v) = 0$ on the line RC in Figure 3A is removed. Then $G(u, v)$ is chosen as a linear function which is negative above the straight line RB and is positive below it. This gives

$$F_2(u, v) = \alpha_2(u - u_0) [u - c_1(v - v_0)^2 - u_4], \quad (16)$$

$$G_2(u, v) = \beta_2[c_4(u - u_0) - (v - v_0)]. \quad (17)$$

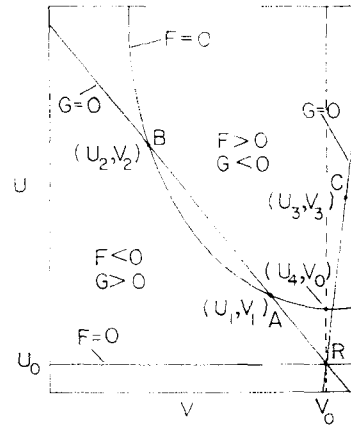


FIGURE 3A. The null isoclines for the reaction terms of the first set of simplified reaction-diffusion equations and regions of the (u, v) plane at which $F_1(u, v)$ and $G_1(u, v)$ are positive or negative. The critical points are again marked A, B and R.

Model 3

The null isoclines for this model are sketched in Figure 3B. Here $G(u, v) = 0$ on the parabola

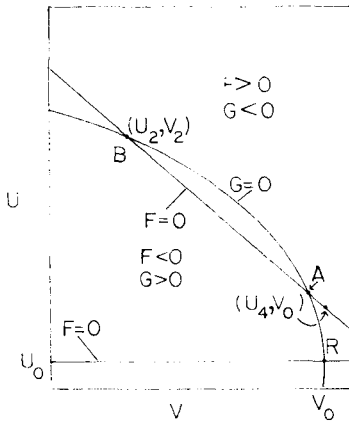


FIGURE 3B The null isoclines for the kinetic system of the third system of simplified reaction-diffusion equations.

through A, B and R whereas $F(u, v) = 0$ on the straight lines AB and $u = u_0$. At fixed v , $F(u, v)$ is quadratic in u with zeros at $u = u_0$ and on the straight line RB, being negative between these values. This gives

$$F_3(u, v) = \alpha_3(u - u_0) [u - u_4 - c_5(v - v_0)], \quad (18)$$

where α_3 is a constant and

$$c_5 = (u_2 - u_4)/(v_2 - v_0). \quad (19)$$

The function $G(u, v)$ is chosen at fixed u to be a linear function of v with a zero on the parabola through RAB. This gives

$$G_3(u, v) = \beta_3[v - (v_0 - c_6(u - u_0)^2)], \quad (20)$$

where β_3 is a constant and

$$c_6 = (v_0 - v_2)/(u_2 - u_0)^2. \quad (21)$$

Model 4

In this case $F(u, v) = 0$ as in model 1 and $G(u, v) = 0$ as in model 3. This gives

$$F_4(u, v) = \alpha_4(u - u_0) (u - c_1(v - v_0)^2 - u_4), \quad (22)$$

$$G_4(u, v) = \beta_4[v - (v_0 - c_6(u - u_0)^2)], \quad (23)$$

where α_4 and β_4 are constants.

RESULTS AND DISCUSSION

In the following investigations of the simplified model equations the values of u_0 and v_0 were set at 2 and 1 respectively, the units of u and v being mM throughout. Thus the rest states of the original four component and two component models are the same as that of the simplified models. In most of the calculations the critical point B was at $(u_2, v_2) = (13, 0.6)$.

Model 1

The value of u_4 was set at 4. This ensures that the system does in fact have a threshold level of potassium ions. Unless $u(x, 0)$ is greater than u_4 for some region in space there will be no sources for potassium ions and the initial stimulus will have no lasting effect of any consequence. The actual thresholds for potassium ion concentration which produce spreading depression in cortical structures are higher than this, though the actual threshold is hard to determine because the eliciting solution is often applied such that the value in the cortex itself is possibly quite different from that in the stimulus. Here, however, we are primarily interested in qualitative rather than precise quantitative theory.

The point C in Figure 3A was set at (10, 1.1), which choice was made simply in order to obtain qualitative behavior of the correct kind. The null isoclines are then completely determined. It was checked that the given choices did make the parabola through (u_2, v_2) and (u_4, v_0) intersect the straight line BR twice. In fact $(u_1, v_1) = (4.45, 0.911)$.

There remains to determine the values of α_1 and β_1 as the same diffusion coefficients were employed as previously. In computing the solutions with the initial data of (8a) and (8b), the boundary conditions $u(0, t) = u(1, t) = u_0$ and $v(0, t) = v(1, t) = v_0$ were always employed. The parameters are so chosen that the wave phenomena occupy a relatively small part of the spatial interval (0, 1) so that the boundary conditions have little effect on the solutions. In the first runs on the computer the values of the constants α_1 and β_1 were so chosen that the magnitudes of $F_1(u, v)$ and $G_1(u, v)$ were about the same as the corresponding $F(u, v)$ and $G(u, v)$ of the reaction-diffusion system (5a)-(5d), with the above mentioned values of the constants. With $u_0 = 2$, $v_0 = 1$ and the above values of u_2 , v_2 , u_3 , v_3 and u_4 , Eqs. (10) and (12) become:

$$F_1(u, v) = \alpha_1(u-2) [u - 56.25(v-1)^2 - 4], \quad (24)$$

$$G_1(u, v) = \beta_1(v - 0.975 - u/80) \times [v - 1 + (u-2)/27.5]. \quad (25)$$

The aim was to find if there were any α_1 and β_1 which would lead to solitary wave solutions.

Various kinds of solutions arose as α_1 and β_1 varied. With $\alpha_1 = 2$ and $\beta_1 = 100$, a "saturating" wave formed with a peak u value of 13 and a corresponding v value of 0.6. The wave profile in space is sketched in Figure 4A. The trajectory at a given point in space as the wave passes is plotted in the (u, v) -plane in Figure 4B. It can be seen that the trajectory leaves the rest point $R = (2, 1) = (u_0, v_0)$ and heads almost directly towards the critical point $(13, 0.6) = (u_2, v_2)$. The latter is evidently a stable critical point.

With $\alpha_1 = 3.12$ and $\beta_1 = 64$, a travelling wave forms which has a very long flat tail at about

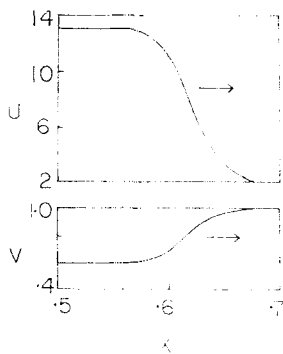


FIGURE 4A The u -component and v -component in the saturating traveling wave obtained for certain parameter values in the first system of simplified equations.

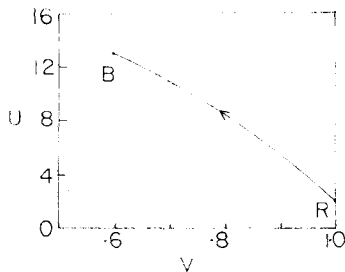


FIGURE 4B The trajectory in the (u, v) -plane at a fixed spatial point as the solitary wave of Figure 4A passes. The upper critical point is at $(13, 0.6)$ which corresponds with the amplitude of the wave.

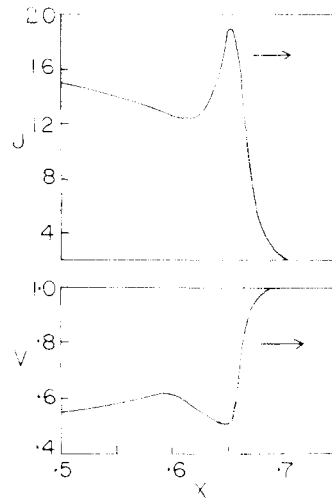


FIGURE 5A A wave solution obtained for model 1 with certain parameter values in which the u -component has a peak at the wave front and an ill-formed tail.

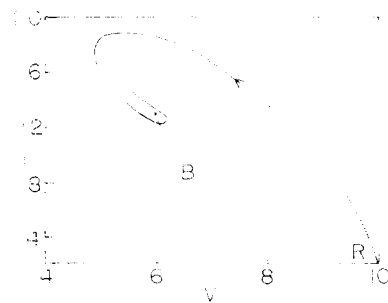


FIGURE 5B Trajectory in the (u, v) -plane corresponding to the wave of Figure 5A.

$(13, 0.6)$. The wave profiles in space for this case are illustrated in Figure 5A and the trajectory in the phase plane shown in Figure 5B. The trajectory emanates from the rest point, manages to go past the point (u_2, v_2) , enters the region of negative F and heads downwards but is attracted towards the critical point B so strongly that it loops around it. What would happen eventually in this case is difficult to ascertain. With $\alpha_1 = 3.6$ and $\beta_1 = 57.6$ a multi-peaked wave started to form so that several loops around B occurred. It was again not feasible to determine whether this would propagate. Due to the behavior of the trajectory in this case the point (u_2, v_2) appeared to behave as an asymptotically stable spiral point.

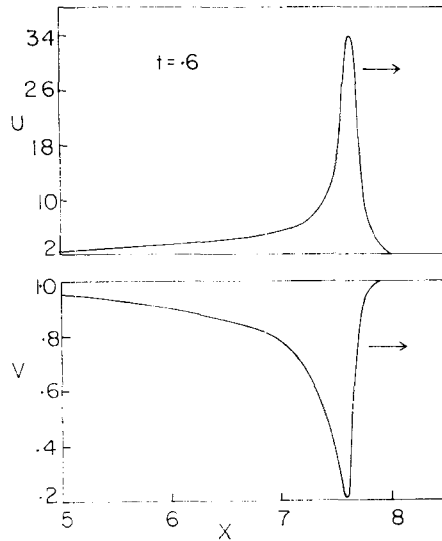


FIGURE 6A The fully developed stable traveling waves obtained for the first simplified system with certain parameter values.

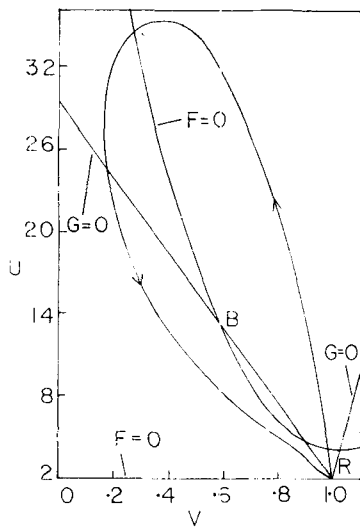


FIGURE 6B Phase plane picture of the solitary wave depicted in Figure 6A.

Finally, the solutions which had been sought, with $\alpha_1 = 3.75$ and $\beta_1 = 54.2$, an apparently stable travelling solitary wave with an amplitude for u of 34 mM and a minimum v value of 0.2 mM was obtained. The wave profile in space is sketched in Figure 6A. The wave fronts are both sharp and

the potassium increases well ahead of the decrease in calcium as is sometimes found experimentally (Kraig & Nicholson, 1978). Also, the return of calcium to its resting value lags behind the return of potassium to its resting value. The solitary wave trajectory is sketched in Figure 6B. The take off from R is nearly vertical which explains why the potassium increase occurs before the calcium decrease. The trajectory goes well past the critical point at $(u_2, v_2) = (13, 0.6)$ bends over and on its descending path manages to avoid the attracting influence of that critical point and return to the rest state R . Thus a complete solitary wave is able to form.

It is concluded that the reaction-diffusion system of model 1 can adequately simulate the behavior of potassium (u) ion and calcium ion (v) concentration as in spreading cortical depression insofar as waves of increased K^+ and decrease Ca^{++} result from a local elevation of K^+ . With $\alpha_1 = 3.75$ and $\beta_1 = 54.2$, the velocity of propagation of the wave of the model 1 is 0.45 space units per unit time. When one allows for the scaling in space and time (the diffusion coefficient of K^+ is about 2.5×10^{-5} cm²/sec and that of Ca^{++} about 1.25×10^{-5} cm²/sec), translating back to original distances and times (see Tuckwell, in press) the velocity is about 4.2 mm/minute. This is in the experimental range of velocities of 2-6 mm/minute.

It was decided to investigate how well this simplified model performed in predicting other experimentally observed phenomena in connection with spreading cortical depression. The first of these is a subthreshold response. With the same α_1 and β_1 that gave solitary waves, the initial data

$$u(x, 0) = 2 + 2 \exp[-\{(x - 0.5)/0.025\}^2], \quad (26)$$

and $v(x, 0) = 1$ were employed. As expected, no wave formed and the initial stimulus died away after causing a slight decrease in calcium ion concentration in the vicinity of the stimulus. Both u and v returned to their resting values eventually. This was a subthreshold response and indicates that the system does in fact have a threshold for the elicitation of solitary waves.

The next experimentally observed phenomenon tested for in the model was the result of a collision of two waves head on. With the same α_1 and β_1 as before, the initial data

$$u(x,0) = 2 + 8 \exp[-\{(x-0.23)/0.025\}^2] + 8 \exp[-\{(x-0.77)/0.025\}^2], \quad (27)$$

and $v(x,0) = 1$ were employed. This corresponds to addition of K^+ (in the form of KCl) at two separate sites of the cortical structure. Solitary waves of K^+ and a corresponding decrease in extracellular Ca^{++} emerged from the centers of the stimuli and collided head on in the middle of the interval $(0,1)$. The collision commenced at $t = 0.52$ and by $t = 0.60$ the wave profiles had merged. The resultant envelope of K^+ collapsed whereas the Ca^{++} grew back up to its original resting level of 1 mM/liter. The waves had thus annihilated each other on collision which is the case for the models described by the systems (1) and (5) and also the experimental collision process. For model 1 described here, the values of v actually went slightly negative in the collision center which could have been circumvented by choosing different values for the constants appearing in the equations.

Suprathreshold concentrations of KCl lead to the emission of a train of waves of spreading depression (see, for example, Mayevsky & Chance, 1974). It is hard to say exactly how the applications of large concentrations of KCl should be incorporated mathematically. It is not clear whether the excess K^+ seeps slowly into the cortex or whether large amounts are cleared by active transport either into cortical cells (neurons and glia) and into the bloodstream. It was decided to test the model's response by employing a constant applied stimulus over a limited region in space. Thus the system of reaction-diffusion equations was integrated numerically with the constraint

$$u(x,t) = u_c, \quad 0.18 \leq x \leq 0.22, \quad t > 0. \quad (28)$$

With $u_c = 5.5$ no waves were emitted from the stimulus. With u_c at 5.8, waves appeared after a considerable delay and for higher values of u_c , waves emerged from the stimulus with varying amplitudes and delays.

Typical results are shown in Figures 7A and 7B. In the first of these, $u_c = 5.8$ and by $t = 2.5$ three waves have formed (only the profiles of u are shown). Only the first wave has the solitary wave shape, the second having a smaller amplitude and the third a wider profile. It seems that the solitary wave cannot repeat because of an extremely slow return of v to v_0 on the solitary wave orbit. With $u_c = 20$, about 4 waves have formed by $t = 1.42$ (Figure 7B) but again only the first has the solitary

wave shape and even here the tail is not well formed. The secondary waves have decaying amplitudes though the distances between them are not too different.

The first model successfully predicts the behavior of the original reaction-diffusion system (and the potassium and calcium ion concentrations as in spreading depression) insofar as it has solitary waves, subthreshold responses and annihilating colliding waves, but it appears not to have a repetitive train of waves in response to a sustained stimulus. Since when $u_c = 5.5$ and less, no waves were emitted and when $u_c = 5.8$ the second wave was quite similar to the first, it is possible that between these values of u_c there is a value or set of values when the time between the first and second waves is sufficient to allow the first wave to form

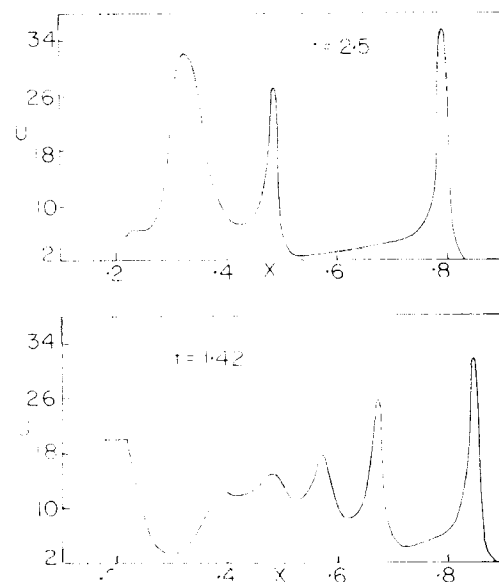


FIGURE 7A The response (u -component only) of the first model system to a sustained stimulus of strength $u_c = 5.8$ applied between $x = 0.18$ and $x = 0.22$. A train of waves emanates from the stimulus but only the first has the solitary wave shape of Figure 6A.

FIGURE 7B As in Figure 7A but with a stronger applied stimulus. Here $u_c = 20$ and the train of waves has a sequence of diminishing amplitudes.

completely and hence give a train of almost identical waves. Other positions of the critical points and other values of the parameters (including

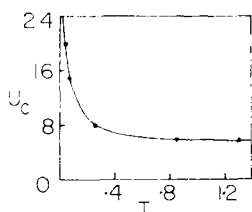


FIGURE 8 A "strength-duration curve" for model 1. The stimulus strength, u_c , is plotted against the time to appearance of the first solitary wave.

the diffusion coefficients) may of course lead to a more perfectly formed set of multiple waves.

It is of interest to see the relationship between the strength of a sustained stimulus and the time of appearance of the (first) solitary wave. When this is done for single neurons with current strength versus its duration the graph is called a "strength-duration" curve. For the first model, with α_1 and β_1 at the above values that gave solitary waves, and with u held in accordance with Eq. (28), the time of appearance was obtained for various values of u_c . The results are plotted in Figure 8. The curve obtained is similar to the strength-duration curve of single neurons. The time to the appearance of a wave of increased K^+ and diminished Ca^{++} tends to infinity as u_c approaches a threshold value between 5.5 and 5.8 mM/liter and tends to some lower limit (reflecting in some sense an absolute refractory period) as u_c becomes infinite.

Model 2

No stable propagating solitary waves were found for this system of reaction-diffusion equations, though a large number of computer runs was performed. With $(u_2, v_2) = (13, 0.6)$, $(u_0, v_0) = (2, 1)$ and $u_4 = 4$ the null isoclines are completely determined. We then have:

$$F_2(u, v) = \alpha_2(u-2)(u-56.25(v-1)^2-4), \quad (29)$$

$$G_2(u, v) = \beta_2((2-u)/27.5 - (v-1)). \quad (30)$$

Depending on the values of α_2 and β_2 , four kinds of behaviors of the numerically computed solutions (apart from subthreshold responses) were found. The first of these, as for example with $\alpha_2 = 4.312$, $\beta_2 = 57.61$, was a saturating wave in response to the initial data of (8a) and (8b). The amplitude of the saturating wave was $u = 13$, $v = 0.6$ and the trajectory in this phase plane and the space profiles

of u and v are as depicted for this kind of behavior in model 1.

The second type of solution encountered occurred for example with $\alpha_2 = 5.999$, $\beta_2 = 57.61$ (that is, α_2 somewhat larger and the same value of β_2). Here a solitary wave started to form but the tail, after appearing, did not come down to u_0 and v_0 but rather oscillated. The profile in space at sometimes appeared as a saturating wave, sometimes with a peak at the wavefront and sometimes with a secondary peak in the tail. The value of $u(0.5, t)$ which is at the center of the applied stimulus, oscillated with a fairly constant period and fairly constant amplitude until $t = 0.6$.

The third kind of behavior was an immediate escalation of u to such large values that a computer overflow was generated; there is the possibility that this corresponds to a solitary wave of extremely large amplitude. This occurred for example with $\alpha_2 = 6.487$ and $\beta_2 = 57.61$.

The fourth kind of behavior was the most interesting, but possibly more from the mathematical than the physiological point of view. A wave of elevated u and depressed v began to form and actually propagate outward from the initial stimulus. The peak of the u -wave remained the same for some time and the tail (at $x = 0.5$) almost came to the resting point (u_0, v_0) . Just as the wave seemed about to properly form and propagate as a solitary wave, instead the amplitude of the wave front and the tail began to grow eventually to the extent that a computer overflow occurred. Smaller time and space steps in the numerical procedure did not obviate the difficulty in forming a solitary wave. It seemed that the instability was real and not due to any errors in the numerical procedures. This kind of behavior occurred for example with $\alpha_2 = 1.666$ and $\beta_2 = 13.75$. If one plots the (u, v) -values in space on this almost developed wave, it can be seen that the loop rather than coming in to R , as it would for a solitary wave, travels almost horizontally at u approximately equal to 3 towards the parabola through AB in Figure 3A. It was not possible by adjusting $F_2(u, v)$ and $G_2(u, v)$ to circumvent this behavior and make the trajectory end up at R . Higher values of u_4 were tried as well as different diffusion coefficients but no solitary waves were obtained. Model 2 was also very sensitive to parameter changes. With $\alpha_2 = 6.487$ and $\beta_2 = 57.61$, an overflow occurred immediately on the computer, whereas with $\alpha_2 = 6.468$ and $\beta_2 = 57.61$, a wave started to form as described in

this paragraph but did not become a properly formed solitary wave.

Model 3

With reference to Figure 3B, the point $(u_0, v_0) = (2, 1)$ was again chosen as the resting state, $(u_2, v_2) = (13, 0.6)$ was chosen as the upper critical point and the point (u_4, v_0) was again set at $(4, 1)$. The null isoclines thus being completely determined, Eqs. (18) and (19) become:

$$F_3(u, v) = \alpha_3(u-2) (u-4 + 22.5(v-1)), \quad (31)$$

$$G_3(u, v) = \beta_3[v - \{1 - 0.0033057(u-2)^2\}]. \quad (32)$$

The initial data of (8a) and (8b) were employed along with the same boundary conditions and with $D_1 = 0.00250$, $D_2 = 0.00125$ to integrate the system numerically. In the first run, with $\alpha_3 = 4$ and $\beta_3 = -15$, the solution became exceedingly large after a few time steps, a computer overflow being the result. Reducing α_3 to 2.667 and leaving β_3 the same gave rise to the appearance of a wave emanating from the stimulus but its amplitude diminished after a short time as it collapsed and did not propagate. Various α_3 and β_3 were tried but a solitary wave was not obtained.

It was decided to shift (u_2, v_2) to $(15, 0.7)$ in order to give the trajectory more "room" to swing around

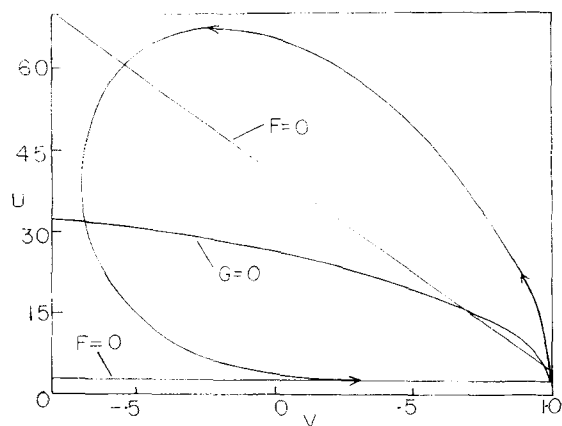


FIGURE 9 The solitary wave trajectory obtained with certain parameter values for the third simplified system of equations. The upper critical point of the kinetic system is at $(15, 0.7)$ and null isoclines are indicated.

on the left of (u_2, v_2) and to make the value of D_2 smaller. The source terms became:

$$F_3(u, v) = \alpha_3(u-2) (u-4 + 36.6667(v-1)), \quad (33)$$

$$G_3(u, v) = \beta_3[v - \{1 - 0.001775(u-2)^2\}]. \quad (34)$$

With $\alpha_3 = 1.2356$, $\beta_3 = -6.4296$, $D_1 = 0.0025$, $D_2 = 0.00075$, solitary waves were finally obtained for this model, the tail of the wave is extremely long and at first it was thought that a solitary wave had not formed because when $u(0.5, t)$ almost reached the resting level 2, it began to grow. It did not grow very much, however, and then started its eventual return to the resting level. The same remarks apply for the second component, v . The solutions had to be computed until $t = 2$ to verify the formation of the solitary waves whereas with model 1 (and 4) the wave had almost completely formed by about $t = 0.7$. The solitary wave trajectory for this model is plotted in Figure 9. It can be seen that the u -wave has a large amplitude of about 70 and the v -wave goes as low as -0.7 . The return to resting state is almost on the line $u = u_0$, as it is in Figure 2. Further properties of this model were not investigated.

Model 4

The rest state was again $(u_0, v_0) = (2, 1)$, the upper critical point was $(u_2, v_2) = (13, 0.6)$ and $u_4 = 4$, whereupon the null isoclines are completely determined. The reaction terms can then be written

$$F_4(u, v) = \alpha_4(u-2) (u-56.25(v-1)^2-4), \quad (35)$$

$$G_4(u, v) = -\beta_4[v - \{1 - 0.0033057(u-2)^2\}]. \quad (36)$$

The reaction diffusion system was integrated numerically with $D_1 = 0.00250$, $D_2 = 0.00125$ with the initial data of (8a) and (8b) and boundary conditions as before. It was quite easy to find solitary waves after only a few trial runs in this case. With $\alpha_4 = 4.258$ and $\beta_4 = 15$, well formed solitary waves quickly appeared. The wave profiles in space are plotted in Figure 10A and the solitary wave trajectory is plotted in Figure 10B. The wave quickly assumes its maximum amplitude and also returns to rest quite rapidly.

With the initial data of Eq. (27) so that waves emanated from $x = 0.23$ and $x = 0.77$, a collision was observed at the center of the interval $(0, 1)$. The profiles at various stages of the collision

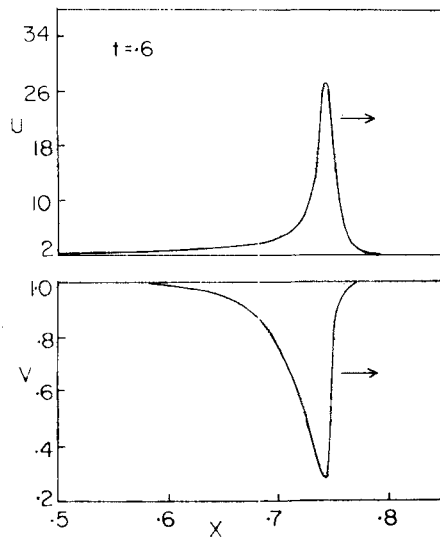


FIGURE 10A The u -component and v -component of the solitary waves obtained in the fourth simplified system of equations.

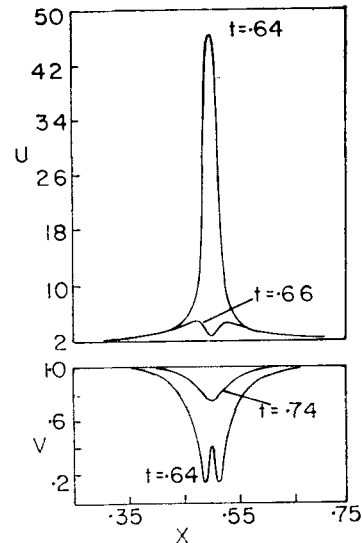


FIGURE 11 Collision profiles of the u -component and v -component at various times for model 4. Two solitary waves have collided at $x = 0.5$ after being elicited by stimuli applied around $x = 0.23$ and $x = 0.77$ at $t = 0$.

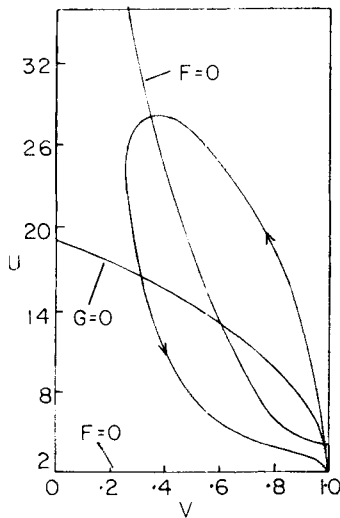


FIGURE 10B The solitary wave trajectory in the (u,v) -plane corresponding to Figure 10A and its relation to the null isoclines and critical points of the kinetic system.

process are shown in Figure 11. At $t = 0.64$ the u -waves have merged to form an envelope which is larger than the solitary wave amplitude and then by $t = 0.66$ collapses to eventually die away to the resting value $u = 2$ over the entire interval. The v -envelope achieves smaller values in the collision

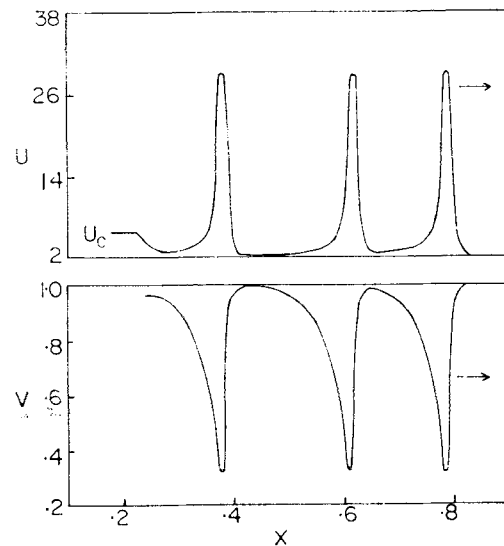


FIGURE 12 Multiple waves for the fourth simplified system emanating from a sustained stimulus of strength $u_c = 6$ applied between $x = 0.18$ and $x = 0.22$.

than in the solitary waves and then collapses to the resting value $v = 1$. Thus, the solitary waves annihilate each other in a head on collision, as they

did experimentally, for the complicated models of the introduction and for model 1.

The response to a sustained stimulus for model 4 consisted of a train of waves of similar amplitudes and shapes emerging from the applied stimulus. With the potassium ion concentration (u) held at $u_c = 6$ in accordance with Eq. (28) the resultant train of waves is sketched in Figure 12. The spacing between the waves does not appear to be uniform. With a larger sustained stimulus, $u_c = 15$, a total of eight waves had formed by $t = 1.8$ as opposed to only 3 in the case of $u_c = 6$. The average spacing between the waves was smaller with the stronger stimulus as is found in experimental studies of multiple waves of spreading depression (Mayevsky & Chance, 1974).

It can be seen that model 4 has very similar properties to the original reaction diffusion systems of the introduction. It has solitary waves, subthreshold responses, multiple waves and annihilation of colliding waves.

SUMMARY AND CONCLUSIONS

The model systems of equations for the behavior of the potassium ion and calcium ion concentrations described in the introduction were previously derived from available physiological and anatomical data with certain extrapolating assumptions for cortical neuronal structures. They successfully predict the approximate quantitative behaviors of these ion concentrations during spreading cortical depression. More precise comparisons of theory and experiment must await the arrival of reliable data on the microanatomical and microphysiological properties of brain structures.

Though those model equations are founded in physiological reality, they are very difficult to analyse. Even the two-component model (5)–(7) has fourteen parameters and the reaction terms contain logarithmic and exponential functions. Hence, it was decided to obtain simpler reaction terms which mimicked the more complicated ones in the relevant parts of the phase plane. This was achieved by locating the null isoclines of the original system and ensuring that their positions and hence those of the critical points of the simpler system were about the same. This resulted in four sets of reaction diffusion equations whose reaction terms contained only polynomials in u and v . The properties of the simplified systems were investi-

gated by numerical integration of the coupled partial differential equations.

The model equations had been so constructed that they all had subthreshold responses to small local elevations of potassium ion concentration. The first model had solitary wave solutions similar to those of the original system when suprathreshold doses of extracellular potassium are applied. With the rest point chosen as the origin this model system may be written

$$u_t = D_1 u_{xx} + a_1 u(u - a_1 v^2 - a_2), \quad (37)$$

$$v_t = D_2 v_{xx} + \beta_1 (v - a_3 u) (v - a_4 u), \quad (38)$$

where $a_1 = c_1$, $a_2 = u_4 - u_0$, $a_3 = c_2$ and $a_4 = c_4$. For this system the solitary waves annihilated each other in a head on collision. Though multiple waves did issue forth from a sustained stimulus of sufficient strength, the train of pulses was not well formed.

For the second system, which can be written

$$u_t = D_1 u_{xx} + a_2 u(u - a_1 v^2 - a_2^2), \quad (39)$$

$$v_t = D_2 v_{xx} + \beta_2 (a_4 u - v), \quad (40)$$

no solitary wave solutions were found and thus the further properties were not investigated.

The third system,

$$u_t = D_1 u_{xx} + a_3 u(u - a_5 v - a_2), \quad (41)$$

$$v_t = D_2 v_{xx} + \beta_3 (v + a_6 u^2), \quad (42)$$

where $a_5 = c_5$ and $a_6 = c_6$, was found to support solitary wave solutions after the position of the upper critical point was shifted and the diffusion coefficient D_2 was changed. The waves had a very large amplitude for the u component and the v -component had (in the original system) negative peak values.

Finally, the fourth system of equations, which can be cast as

$$u_t = D_1 u_{xx} + a_4 u(u - a_1 v^2 - a_2), \quad (43)$$

$$v_t = D_2 v_{xx} + \beta_4 (v + a_6 u^2), \quad (44)$$

seemed to have the desired properties for a simplified model designed to mimic the original complicated system. In addition to subthreshold responses, the system possessed well formed stable solitary waves which annihilated each other in a

head on collision. Also, the response to a sustained stimulus consisted of a train of well-formed waves. It is possible that with certain choices of parameters in this model the v component could go negative and the u component could take on large values which would not occur in the original complicated system or in an experimental situation. To prevent these possibilities one would have to introduce much more complicated reaction terms which would defeat the purpose of seeking a simplified system of equations. It has been demonstrated that the fourth model shares, for the parameter values employed, the properties of the original complicated system.

REFERENCES

- Brinley, F. J., Kandel, E. R., & Marshall, W. H. Potassium outflux from rabbit cortex during spreading depression. *Journal of Neurophysiology*, 1960, **23**, 246-256.
- Higashida, H., Mitari, G., & Watanabe, S. A comparative study of membrane potential changes in neurons and neuroglial cells during spreading depression in the rabbit. *Brain Research*, 1974, **65**, 411-425.
- Kraig, R. P. & Nicholson, C. Extracellular ionic variations during spreading depression. *Neuroscience*, 1978, **3**, 1045-1059.
- Leao, A. A. P. Spreading depression of activity in the cerebral cortex. *Journal of Neurophysiology*, 1944, **7**, 359-390.
- Lees, M. In: *Numerical Solution of Partial Differential Equations*, W. F. Ames (Ed.), New York: Barnes and Noble, 1969, p. 193.
- Llinas, R., Steinberg, I. Z., & Walton, K. Presynaptic calcium currents and their relation to synaptic transmission; voltage clamp study in squid giant synapse and theoretical model of the calcium gate. *Proceedings of the National Academy of Science, U.S.A.*, 1976, **73**, 2918-2922.
- Mayevsky, A. & Chance, B. Repetitive patterns of metabolic changes during cortical spreading depression of the awake rat. *Brain Research*, 1974, **65**, 529-533.
- Nicholson, C., Bruggencate, G. ten, Steinberg, R., & Stockle, H. Calcium modulation in brain extracellular microenvironment demonstrated with ion-selective micropipette. *Proceedings of the National Academy of Science, U.S.A.*, 1977, **74**, 1287-1290.
- Nicholson, C. & Kraig, R. P. The behavior of extracellular ions during spreading depression. In: *The Application of Ion-Selective Electrodes*, T. Zeuthen (Ed.), Amsterdam: Elsevier/North Holland, 1980 (in press).
- Nicholson, C., Bruggencate, G. ten, Stockle, H., & Steinberg, R. Calcium and potassium changes in extracellular microenvironment of cat cerebellar cortex. *Journal of Neurophysiology*, 1978, **41**, 1026-1039.
- Quastel, D. M. J. Excitation-secretion coupling at the mammalian neuromuscular junction. In: *Synaptic Transmission and Neuronal Interaction*, p. 23, New York: Raven Press, 1974.
- Rosenthal, M. & Somjen, G. Spreading depression, sustained potential shifts, and metabolic activity of cerebral cortex of cats. *Journal of Neurophysiology*, 1973, **36**, 739-749.
- Sugaya, E., Takato, M. & Noda, Y. Neuronal and glial activity during spreading depression in the cerebral cortex of cat. *Journal of Neurophysiology*, 1975, **38**, 822-841.
- Tuckwell, H. C. Predictions and properties of a model of potassium and calcium ion movements during spreading cortical depression. *Intern. Journal of Neuroscience*, 1980a, **10**, 145-164.
- Tuckwell, H. C. Ion and transmitter movements during spreading cortical depression. *International Journal of Neuroscience* (in press).
- Tuckwell, H. C. & Miura, R. M. A mathematical model for spreading cortical depression. *Biophysical Journal*, 1978, **23**, 257-276.
- Van Harreveld, A. & Fifkova, E. Mechanisms involved in spreading depression. *Journal of Neurobiology*, 1973, **4**, 375-387.
- Vyskocil, F., Kriz, N., & Bures, J. Potassium-selective microelectrodes used for measuring the extracellular brain potassium during spreading depression and anoxic depolarization in rats. *Brain Research*, 1972, **39**, 255-259.